Ultrasound-Assisted Coating of Nylon 6,6 with Silver Nanoparticles and Its Antibacterial Activity

N. Perkas,[1] G. Amirian,[1] S. Dubinsky,[2] S. Gazit,[2] A. Gedanken[1]

[1]*Department of Chemistry and Kanbar Laboratory for Nanomaterials, Bar-Ilan University Center for Advanced Materials and Nanotechnology, Bar-Ilan University, Ramat-Gan, 52900, Israel*
[2]*Nilit, Limited, P.O. Box 276, Migdal Haemek 23102, Israel*

Received 23 February 2006; accepted 23 February 2006
DOI 10.1002/app.24728
Published online in Wiley InterScience (www.interscience.wiley.com).

ABSTRACT: A silver/nylon 6,6 nanocomposite containing 1 wt % metallic silver has been produced from an aqueous solution of silver nitrate in the presence of ammonia and ethylene glycol by an ultrasound-assisted reduction method. The structure and properties of nylon 6,6 coated with silver have been characterized with X-ray diffraction, transmission electron microscopy, scanning electron microscopy, energy-dispersive X-ray, X-ray photoelectron spectroscopy, Raman spectroscopy, and diffused reflection spectroscopy measurements. The nanocrystals of pure silver, 50–100 nm in size, are finely dispersed on the polymer surface without damaging the nylon 6,6 structure. This silver–nylon nanocomposite is stable to many washing cycles and thus can be used as a master batch for the production of nylon yarn by melting and spinning processes. The fabric knitted from this yarn has shown excellent antimicrobial properties. © 2007 Wiley Periodicals, Inc. J Appl Polym Sci 104: 1423–1430, 2007

Key words: coatings; nanocomposites; particle size distribution

INTRODUCTION

The antibacterial properties of silver have been known and used for centuries.[1] A unique and available source of silver has long been mineral salts. The development of nanotechnology opens up a new opportunity for silver delivery by the formation of organic–inorganic nanocomposites combining various properties of polymers with antibacterial activity.[2–5] The incorporation of silver nanoparticles into polymers is of great interest for many researchers because of the widespread applications of these materials in food processing, medical equipment, agriculture, biochemistry, textiles, and so forth.[6–10] To achieve the optimum antibacterial effect of nanocomposite fibers, a high concentration of silver ions must be available in the solution. Despite the small number of silver ions released from metallic silver nanocrystals, about 30 times less than that from silver complexes (e.g., silver sulfadiazine), a more rapid microbe-killing curve has been observed with nanocrystals.[11] Pure silver delivery systems also have a positive influence on wound healing. On the other hand, silver complexes demonstrate a negative effect on this process. This difference exists because the small Ag(0) clusters of nanocomposites can release other silver species besides silver ions, such as silver atoms,[11,12] which may be partly or wholly responsible for the effective antibacterial properties of pure-silver-containing polymers.[12]

The principal requirements for the synthesis of metal–polymer nanocomposites are small dimensions, a regular shape, and a uniform size distribution of the metal (silver in this study) nanoparticles. Different methods have been assayed for the incorporation of pure silver into polymers such as *in situ* polymerization,[13–15] the sol–gel technique,[16] and a laser ablation method.[17] The agglomeration of metallic silver can be prevented by the addition of surfactants such as mercaptosuccinic acid,[15] sodium dodecyl sulfonate, and *n*-dodecyl mercaptan[17] or amphiphilic hyperbranched macromolecules[14] as stabilizing agents. However, most nanocomposites derived from polymerization-based techniques should be exposed to the melt-processing stage and should undergo dilution in additional polymeric material to create a bulk polymer. Only limited information is available concerning the preparation of silver–polymer master batches and their incorporation into industrial polymers by melt compounding.[18,19] Thus, the synthesis of well-dispersed silver–polymer nanocomposites for the preparation of nylon fibers with antibacterial properties is still a very important task.

Sonochemical irradiation has been proven to be an effective method for the synthesis of nanophase materials as well as the deposition and insertion of nanoparticles onto and into mesoporous ceramic and polymer supports. The advantage of this method is the homogeneous coating of small nanoparticles with a narrow size distribution.[20–22] In previous publications, we

Correspondence to: A. Gedanken (gedanken@mail.biu.ac.il).
Contract grant sponsor: Israeli Ministry of Commerce and Industry, through the MAGNET program to the NFM project.

have reported on the preparation of amorphous silver of about 20 nm in size[23] and on the deposition of homogeneously distributed silver nanoparticles with an average diameter size of $\sim$ 5 nm on the surface of silica submicrospheres with the aid of ultrasound irradiation.[24] The reactions were carried out in an aqueous solution under an argon/hydrogen (95 : 5) atmosphere with silver nitrate as a precursor. However, in one example,[24] a high concentration of ammonia was required to produce silanol groups on the SiO_2 surface to achieve the homogeneous coating of the support with silver nanoparticles. These conditions are not suitable for a nylon support because they can cause irreversible changes in the nylon's structure. Sonochemistry has also been employed for the insertion of silver nanoparticles into mesoporous silica in water solutions containing small amounts of isopropyl alcohol.[25] However, according to transmission electron microscopy (TEM) measurements, silver particles obtained by this method are in the wide range of 10–100 nm with a tendency to aggregate.

The polyol reduction method has been used previously for the preparation of finely dispersed silver nanoparticles. This process involves the reduction of soluble silver species by ethylene glycol (EG) in the presence of suitable protective agents, such as poly (vinyl alcohol), polyacrylate, and poly(vinyl pyrrolidone) (PVP), which can prevent the agglomeration of nanoparticles at relatively low temperatures (6–120°C).[26,27] A control-sized (6–7 nm) colloid silver–PVP nanocomposite has been obtained by the sonochemical modification of the polyol reduction process with PVP as a protective agent. This system can be used in polycarbonate as a UV absorber and a color filter.[28] Similar data for the synthesis of a silver–nylon nanocomposite have not been found in the literature.

This work is the first report on the preparation of a silver–nylon nanocomposite that can be used as a master batch for antibacterial nylon fibers. The incorporation of silver into nylon 6,6 has been carried out by ultrasound irradiation with the addition of EG as a polyol reducing agent. The structure of the silver–nylon composite has been characterized by a series of physicochemical methods, such as X-ray diffraction (XRD), TEM, scanning electron microscopy (SEM), energy-dispersive X-ray (EDX) analysis, X-ray photoelectron spectroscopy (XPS), diffused reflection optical spectroscopy (DRS), and Raman spectroscopy. The silver–nylon composite has been used as the master batch at the Nilit, Ltd. (Migdal Haemek, Israel), pilot plant for spinning nylon yarn.

EXPERIMENTAL

Materials

All the chemical reagents of chemical grade were purchased from Sigma-Aldrich (Steinheim, Germany) and used without further purification. The nylon 6,6 chips were supplied by Nilit. The average size of the cubic grains was 3 mm. Several parameters were changed to obtain the best conditions for the coating of silver nanoparticles on the polymer: the ultrasound power, solution temperature, reaction time, and concentrations of the reagents. The optimal results representing a typical experiment were as follows. Five grams of nylon 6,6 chips was added to a 0.02*M* $AgNO_3$ solution of water and EG (10 : 1 v/v) in a 100-mL sonication flask. The reaction mixture was then purged under Ar for 1 h to remove traces of O_2/air and irradiated for 2 h with a high-intensity ultrasonic horn (Ti horn, 20 kHz, 600 W at 70% efficiency) under the flow of an Ar–H_2 mixture (95 : 5). A 25 wt % aqueous solution of ammonia (NH_4OH/$AgNO_3$ molar ratio = 2 : 1) was added to the reaction slurry during the first 10 min of sonication. The sonication flask was placed in a cooling bath with a constant temperature of 30°C during the sonication. At the end of the sonication process, the color of the polymer chips changed from white to bright gray (Fig. 1). The product was washed thoroughly first with water to remove the traces of ammonia and then with ethanol and was dried *in vacuo*. The as-prepared silver–nylon composite was used as a master batch at the Nilit partially oriented yarn (POY) pilot plant, at which nylon 6,6 27/7 (decitex) yarn containing 0.1 wt % silver was spun. This yarn was tested at Aminolab, Ltd. (Nes-Ziona, Israel), for antimicrobial activity according to AATCC Test Method 100-1993.

Measurements

The silver content in the polymer was determined by volumetric titration with KSCN according the

Figure 1 Photograph of nylon chips before and after sonochemical coating with silver and silver–nylon fibers spun from the silver–nylon composite. [Color figure can be viewed in the online issue, which is available at www.interscience.wiley.com.]

Foldgard method, the first step being the dissolution of the silver in HNO_3.[29] In addition, elemental analysis was also carried out by EDX measurements on a JEOL JSM 840 scanning electron microscope (Tokyo, Japan). The XRD patterns were obtained with a Bruker D8 diffractometer (Karlsruhe, Germany) with Cu Kα radiation. The particle size and morphology of the nanocomposite were observed by electron microscopy with a JEOL JEM 100 TEM microscope and a JEOL JEM 5600 for SEM measurements (Tokyo, Japan). The valence state of silver was determined by XPS on a Kratos Axis HS spectrometer (Manchester, UK) with Al Kα radiation. The C1s with binding energy (E_b = 285.0 eV) peak was chosen as a reference line for the calibration of the energy scale. The spectroscopy studies also included diffusion reflection spectroscopy and Raman studies. The diffusion reflection optical spectra were recorded on a Cary 100 Scan UV spectrometer (Melbourne, Australia) in a 200–600-nm wavelength range. The Raman spectra were collected with a JY Horiba Olympus Bx41 spectrometer (Longjumeau, France) with a 514-nm Ar^+-ion-laser excitation source.

RESULTS AND DISCUSSION

Effect of the reagent concentration

The different compositions used in the reaction are presented in Table I. Differences in the silver concentrations in the polymer obtained by volumetric titration and EDX have been detected. The silver content determined by EDX is always larger than the titration results. The higher numbers obtained by EDX can be explained as follows. The chemical analysis monitors the total silver content. The HNO_3 treatment is performed in water at the boiling temperature for 40 min and fully dissolves the metallic silver. The titration results correspond, therefore, to the total content of silver in the nylon. On the other hand, most silver nanoparticles measured by electron-dispersive X-ray analysis are localized on the outer surface of the nylon chips. Although the penetration depth of EDX is about 500 nm, it still probes mostly the outer part of the nylon chip, and this is the reason that a higher concentration of silver is obtained by EDX.

TABLE I
Optimization of the Reagent Composition for Silver–Nylon Synthesis

Sample	$AgNO_3$ (mol/L)	EG (mL)	NH_4OH (mL)	Silver (wt %)	
				Titration	EDX
1	0.02	—	7	0.12	0.15
2	0.02	10	—	0.21	0.25
3	0.02	10	7	0.46	0.49
4	0.02	10	1	0.75	0.80
5	0.02	10	0.3	1.00	1.23
6	0.02	25	0.3	1.02	1.20
7	0.02	5	0.3	0.69	0.73
8	0.05	10	0.75	1.05	1.25
9	0.01	10	0.15	0.58	0.60

From the analytical results, it is clear that the presence of both EG and ammonia is necessary to obtain a relatively high concentration of silver in the nylon (samples 3–9). We started with a 40-fold molar excess of ammonia according to the previous data,[24] which demonstrated that the attachment of highly dispersed silver nanoparticles to the negatively charged surface of a silica support takes place through the formation of the $[Ag(NH_3)_2]^+$ complex. However, the high concentration of ammonia leads to changes in the polymer's color, converting it from white to brown-yellow. It also causes additional difficulties in washing the product after the reaction (samples 1 and 3). In the absence of ammonia, the reduction process was very slow, and no significant coating of the polymer was monitored (sample 2). Thus, the optimal concentration of ammonia is a 2 : 1 molar ratio of ammonia to silver (0.3 mL of NH_4OH in 100 mL of a working solution). This ratio corresponds to the formation of a $[Ag(NH_3)_2]^+$ complex.

We have also found that EG not only acts as a polyol reduction agent, as in the preparation of silver–polymer composites,[26–28] but also promotes the anchoring of silver nanoparticles to the surface of nylon by interaction with the surface functional groups. We reached this conclusion because the reduction of Ag^+ in solution was also observed without the addition of EG. Nevertheless, in the absence of EG, we did not get any noticeable coating of the polymer with silver. A comparison of samples 1 and 3 in Table I indicates the same thing, that is, the role of EG in helping to deposit larger amounts of silver on the surface. Table I also shows that for a high concentration of EG, the solution's viscosity increases, and this causes some difficulties in the sonication reaction (sample 6). For low concentrations of EG, the silver coating on nylon is not homogeneous. Thus, the optimal concentration of EG corresponds to 10 vol % of the working solution.

We have also tested how the amount of anchored silver is dependent on the content of $AgNO_3$ in the solution. An increase in the silver concentration to more than 0.02 mol/L does not lead to more metallic silver coating on the polymer surface. In addition, when a high concentration of $AgNO_3$ was used, a large amount of metallic silver precipitated at the bottom of the sonication cell, and this required additional steps for separation. On the other hand, the silver content decreased in the nanocomposite when low concentrations of $AgNO_3$ (0.01 mol/L; sample 9) were used. The optimal chosen conditions corre-

spond to sample 5, resulting in 1 wt % silver in the composite. Sample 5 yielded the maximum concentration of silver deposited on the surface of nylon 6,6. Hereafter, all the characterization data apply to sample 5. This silver-coated nylon composite was exposed to several washing procedures in water at elevated temperature (60–80°C). The silver concentration did not change, even after 10 washing cycles. These results demonstrate the high stability of coating silver on nylon, a unique property of sonochemical coating. The already available commercial antibacterial master batches usually consist of 20–30 wt % functional silver-based additives, whereas the concentration of silver is up to 10 wt %.

Structure and morphology of the silver–nylon composite

A TEM image of silver particles obtained during the sonication process that are not anchored to the nylon surface is presented in Figure 2. The figure shows that the silver particles are pseudospherical in shape with a tendency to agglomerate. The average size of a single particle is about 50–100 nm, although smaller particles have also been found. For some particles and groups, it is possible to detect a surrounding outer layer that prevents the particles from further agglomeration. This stabilizing layer is perhaps formed as a result of the partial polymerization of EG during sonication. The cutoff section technique for the nylon chips allows the observation of the distribution of silver particles inside the polymeric chip (Fig. 3). The average size of the particles is about 20 nm, but some aggregates of 100 nm have also been detected.

The SEM method provides an image of the silver particle distribution on the nylon surface (Fig. 4). The polymer is uniformly coated by silver nanoparticles 50–100 nm in diameter. Large agglomerates are not observed on the composite surface. This means that noticeable agglomeration takes place only for the silver powder that is not anchored to the nylon's surface. Bubbles are known to collapse near the surface of solid particles. Microjets and shock waves are among the aftereffects of bubble collapse. The ultrasound waves promote, with the help of the microjets, the fast migration of silver nanoparticles formed during the sonication process to the nylon's surface. Thus, the silver clusters are homogeneously distributed on the polymer surface as individual, nonaggregated particles. The silver nanoparticles impinge on the nylon surface at such a high speed that they might cause its melting. That is why the particles strongly adhere to the surface. We also attribute the strong bonding of the particle to the surface to its

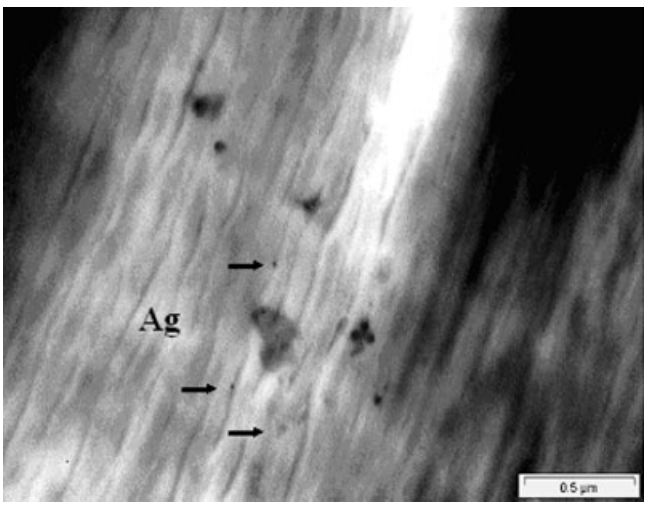

Figure 3 TEM image of a silver–nylon composite (cutoff section).

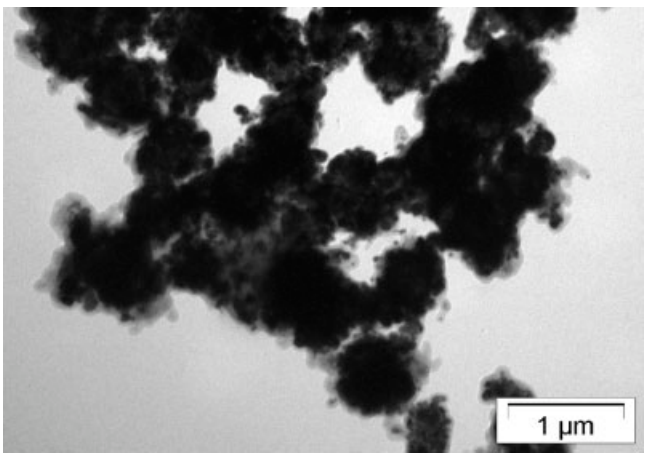

Figure 2 TEM image of silver obtained by the sonication process.

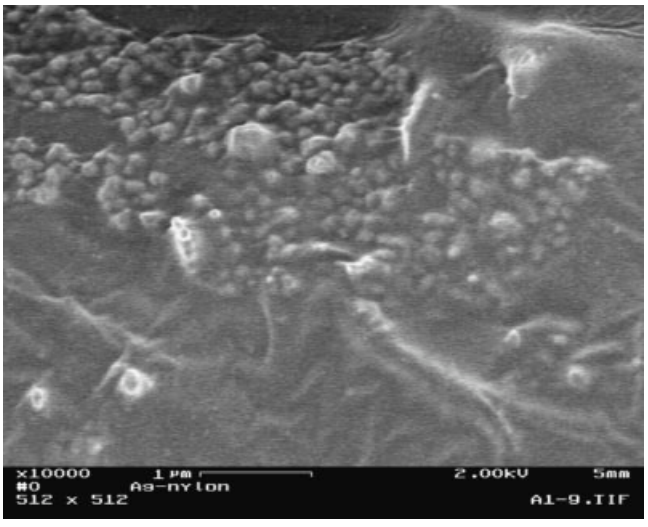

Figure 4 SEM image of a nylon surface coated with silver.

interaction with functional groups of nylon 6,6. This interaction prevents the aggregation of the silver particles. Because of the very high speed at which the particles are thrown at the surface, the smaller silver particles are able to penetrate the surface and are distributed inside the polymeric chip (Fig. 3).

The XRD patterns (Fig. 5) of the product demonstrate that the silver deposited on nylon is crystalline in nature, and the diffraction peaks match those of the cubic silver phase in the Joint Committee for Power Diffraction Studies (JCPDS) database (PDF 4-783). According to the Scherrer formula, the crystalline size of silver nanoparticles is 80 nm, which is in good agreement with the electron microscopy measurements.

Spectroscopy studies

The XPS spectrum of a silver–nylon composite confirms that the silver is in a zero oxidation state. The peaks observed in the energy region of the silver 3d transition are symmetric and centered at 367.9 and 373.9 eV, and both correspond to the database values of Ag(0) (Fig. 6). Changes in the C1s or N1s peaks, which would have provided more evidence for the silver–nylon interaction, could not be discerned in the spectrum.

Additional information concerning the silver–nylon interaction has been obtained from optical and Raman spectroscopy. The nanocrystalline silver-coated polymer displays an optical reflectance spectrum due to collective surface plasma resonance.[30] This optical property is sensitive to many factors, such as the geometry parameters, microstructure, and interaction with the surrounding matrices.[17,28,30] DRS of silver particles collected from the solution after the sonication process and of the silver–nylon composite shows a reflection peak centered at 330 nm (Fig. 7). The location of this peak in DRS is strongly blueshifted in comparison with the usually registered optical reflection of silver nanoparticles at about 400 nm.[17,28] However, the appearance of a silver absorption–reflection peak

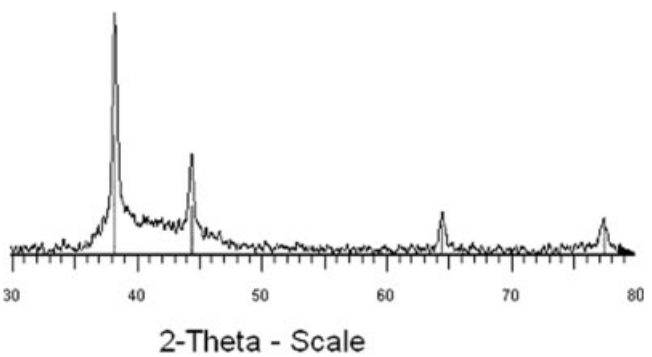

Figure 5 XRD diffraction patterns of a silver–nylon composite.

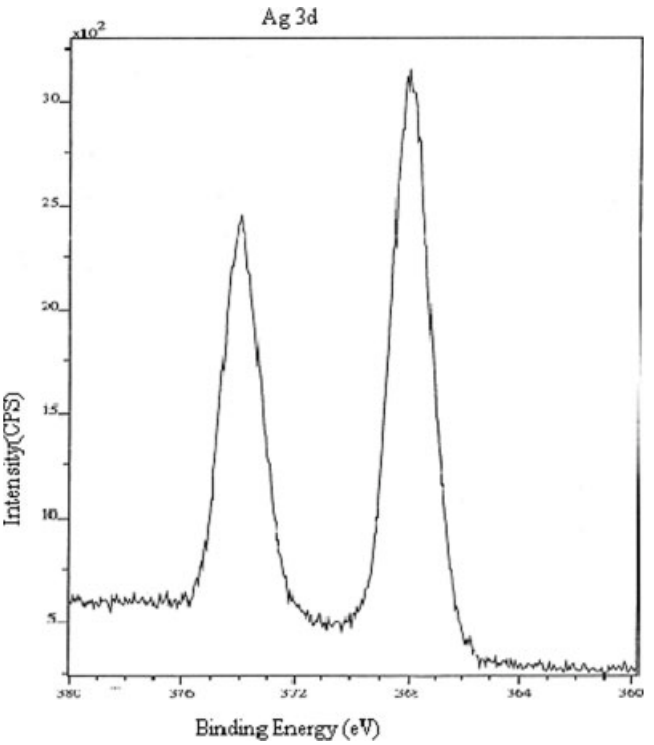

Figure 6 XPS spectrum of a silver–nylon composite.

at about 320–330 nm with a simultaneous decrease in the intensity of the 400-nm band is not new and has already been reported.[31,32] In these previous reports, the large blueshift was attributed to the particle size diminution in the silver colloid. Moreover, theoretical calculations of the energy of the plasmon band of Ag(0) resulted in locating its absorption at about 340 nm.[33] A DRS spectrum similar to our curve was obtained for nanocrystalline silver with a particle size of 50 nm.[34] The authors noted that a decrease in the particle size also led to less intense optical reflectance. Figure 6 illustrates that the incorporation of silver

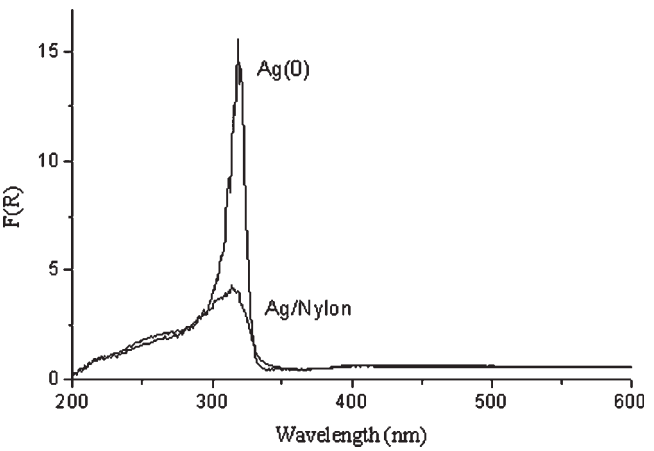

Figure 7 Diffused reflection spectra of a silver–nylon composite.

onto and perhaps into the nylon decreases the peak's intensity. This can again be related to the lack of agglomeration in the silver-coated nylon, leading to smaller silver particles than the separated silver nanoparticles remaining in the solution after sonication. This result is in agreement with the difference in the silver particle size obtained by TEM and SEM studies of the silver–nylon composite and separated silver particles (Figs. 3 and 4). Nevertheless, the lower intensity can also be due to the low silver concentration on the polymer.

Raman spectroscopy has been applied to the characterization of polyamide bonds and to provide knowledge about the structure, bonding nature, and changes upon their reaction.[35] At the same time, Raman spectroscopy is widely used for investigating silver nanocrystalline systems.[36–38] The Raman spectra of the original nylon chips before and after a sonochemical treatment (without silver) are presented in Figure 8(I). Here we see the characteristic bands at 3330 and 1635 cm^{-1}, which are correlated to the stretching vibrations of N—H and C=O,

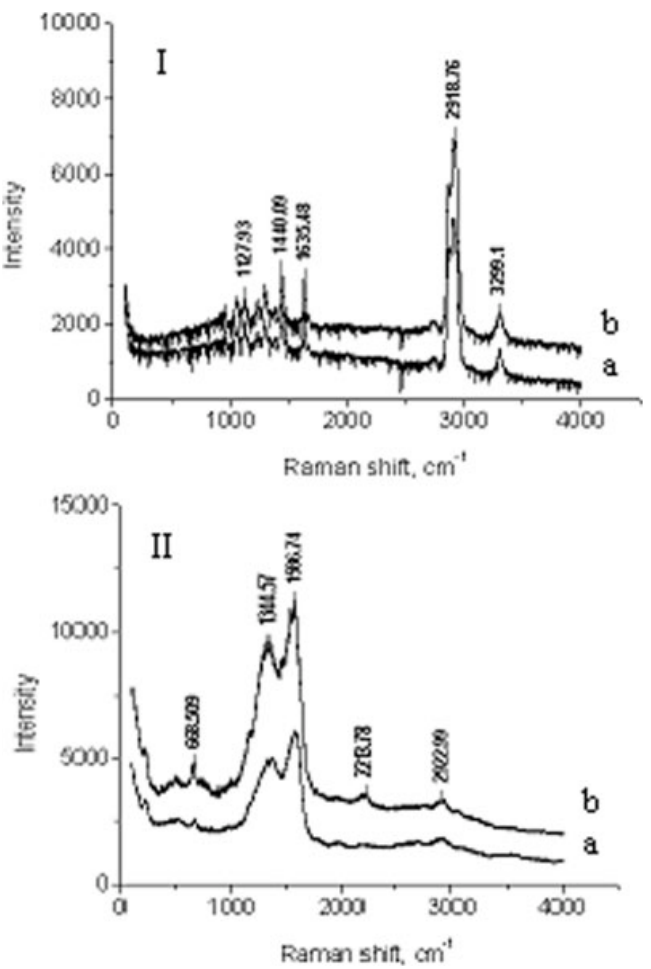

Figure 8 Raman spectra of (I-a) nylon chips (raw material), (I-b) nylon after sonication, (II-a) pure silver, and (II-b) a silver–nylon composite.

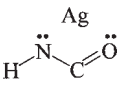

Scheme 1 Bonding of silver to the amide group.

respectively. These two bands are characteristic of nylon 6,6.[35] The strong peaks at 2918 cm^{-1} and at the 1440-cm^{-1} band correspond to hydrogen stretching vibrations in the C—H group. The number of weak lines at 800–1300 cm^{-1} can be related to C—C stretching vibrations. Thus, we do not observe any special influence of ultrasound wave treatment on nylon 6,6. The bands at 3330 and about 1640 cm^{-1}, which are defined in the literature as the fingerprints of nylon 6,6, can both be observed in the raw and ultrasound-treated polymer spectra. After the incorporation of silver into the polymer, the intensity of the peaks at 3330 (N—H) and 1640 cm^{-1} (C=O) is appreciably weakened in comparison with the peaks appearing at 1344 and 1586 cm^{-1}, as demonstrated in Figure 8(II). These last two peaks (1344 and 1586 cm^{-1}) have been observed both in pure silver nanoparticles separated from the sonication solution and in the silver–nylon composite and are characteristic of silver nanoclusters.[38] These peaks are very intense and overlap the region of the C=O vibrations in nylon 6,6. Thus, it is not possible to observe the 1640-cm^{-1} band in the spectrum. The peak at 668 cm^{-1} also appears in spectra of both the pure silver and the silver–nylon composite. All three peaks can therefore serve as indicators for the presence of silver nanoparticles in the polymer. The 668-cm^{-1} band has been observed in silver colloids stabilized by PVP and in silver–polymer-coated paper.[36,37] The weakening of the 3330-cm^{-1} band and perhaps the disappearance of the 1640 band (if not disappearing, then at least weakening) can be explained as being due to the silver bonding to the polymer surface via the amide group. The nonbonding electrons of the carbonyl and nitrogen in the amide moiety are donated to the metallic silver. We can thus envision a four-atom complex of H—N—C=O for silver. The formation of such bonding (Scheme 1) might explain why 10 laundering cycles of the coated particles did not affect the silver concentration at all.

The silver–nylon nanocomposite was used as a master batch for spinning nylon 6,6 POY 27/7 (decitex) yarn containing 0.1 wt % silver. The pellets of the master batch were combined with a stream of neat nylon 6,6 pellets at the feed hooper and thus were diluted to the required concentration in the yarn. The fabric was knitted from this yarn on a one-feed knitting machine. The POY melt-spinning process is a well-known technology for producing manmade yarn. Nylon, polyester, and other synthetic yarns are manufactured by this method. The schematic presentation

of the melt-spinning process is given in Figure 9. Polymeric material is melted in the extruder and transported though a heated manifold toward positive-action, highly precise metering pumps. The pumps release an accurate amount of the polymeric melt that forms the separated filaments by passing through a special die: the spinneret. The separated filaments are then quenched by cool air and collected together in a finishing die, in which a special antistatic emulsion coats the filaments. The freshly formed yarn is wound on sleeves at a high speed of 4200–4800 mps.

The silver–nylon master batch was mixed in the melt with pure nylon 6,6 to reduce the silver concentration to the level currently used for antibacterial underwear applications, that is, 0.1 wt % silver. The standard antimicrobial test demonstrated the high efficiency of this material against microorganisms. The log reduction test showed that the four-level bacterial number drops after 18 h. These results are applicable to Gram-positive (*Staphylococcus aureus*) and Gram-negative (*Pseudomonas aeruginosa*) bacteria.

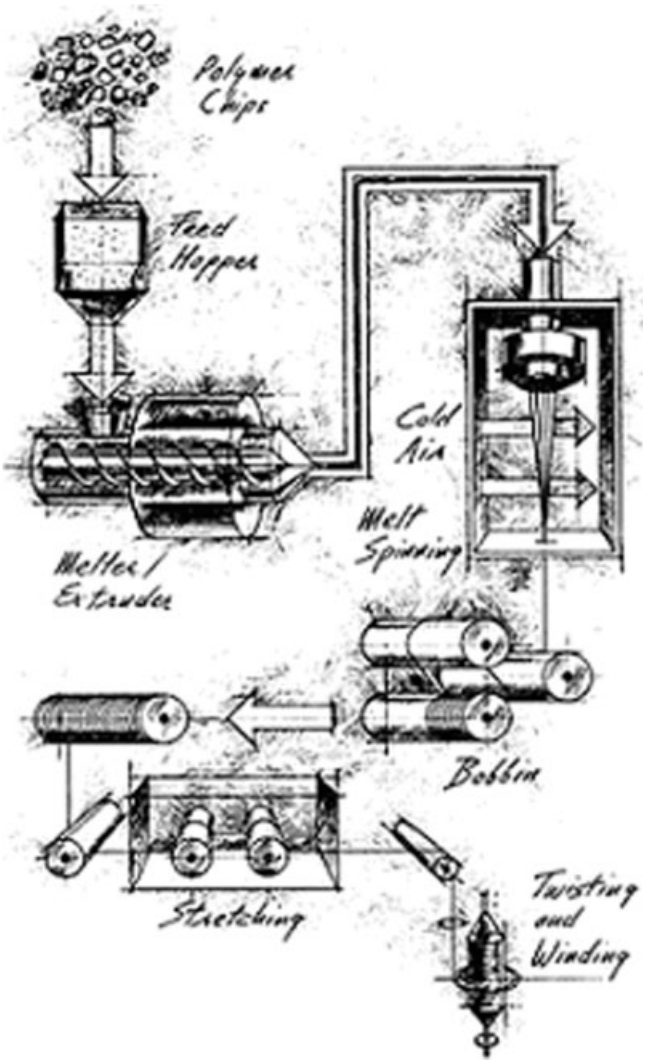

Figure 9 Scheme of the melt-spinning process.

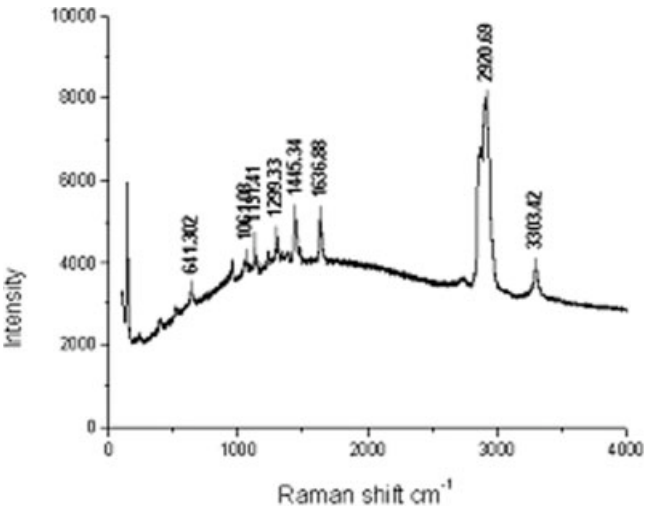

Figure 10 Raman spectrum of silver–nylon yarn.

However, during the production of the yarn, the color changed from light silver to light yellow (Fig. 1). A similar change from a silvery white to a golden yellow was also demonstrated.[34] Reference 34 attributed the color change from light silver to light yellow to the decrease in the silver particle's size from 50 to 35 nm. The authors[34] further explained that with a decrease in the particle size, the spectrum was depleted, mostly at the blue end, relatively less in the green region, and least in the red region. This resulted in the change to a golden yellow. To check the reason for the color change, we recorded the Raman spectrum of silver–nylon yarn (Fig. 10). Here the same characteristic peaks at 3330 and 1640 cm^{-1} observed for the original nylon 6,6 can be seen. The peaks at 2920 and 1445 cm^{-1}, corresponding to hydrogen stretching vibrations in the C—H group, can also be observed. If the Raman spectrum of the yellow yarn is compared with that of the original polymer in Figure 8(I), the main difference observed is in the low energy range of the spectrum, namely, the small bands at 640 cm^{-1} and at lower wave numbers. According to our interpretation, the bands observed for the silver–nylon composite in Figure 8 (II) can indicate the presence of silver nanoparticles in the polymer.

CONCLUSIONS

Nylon 6,6 has been coated with silver nanoparticles by the simple and efficient method of ultrasound irradiation. The incorporation of metallic silver into 3-mm chips has reached 1 wt % silver. The coating is stable, and the concentration of silver in the polymer does not change after 10 washing cycles. The physical and chemical analysis has shown that nano-

crystalline pure silver, 50–100 nm in size, is finely dispersed on the polymer without any damage to the structure of nylon 6,6. Smaller silver nanoparticles about 20 nm in size penetrate the surface and are distributed inside the polymer grains. This silver–nylon nanocomposite can be used as a master batch for the production of nylon yarns by melting and spinning processes. The fabric woven from this yarn has demonstrated very good antimicrobial properties.

References

1. Searle, A. The Use of Metal Colloids in Health and Disease; Sutton: New York, 1919; p 75.
2. Birringer, R. Mater Sci Eng 1989, 117, 34.
3. Shukla, S.; Seal, S.; Schwartz, S.; Zhou, D. J Nanosci Nanotechnol 2001, 1, 417.
4. Zhang, J.; Wang, B. J.; Ju, X.; Liu, T.; Hu, D. Polymer 2001, 42, 3967.
5. Liu, X.; Wu, Q. Polymer 2002, 43, 1933.
6. Wright, J.; Lam, K.; Burrel, R. Am J Inf Control 1998, 226, 572.
7. Mackeen, P. C.; Person, S.; Warner, S. C. Antimicrob Agents Chemother 1987, 31, 93.
8. Adams, A. P.; Santachi, E. M.; Mellencamp, M. A. Vet Surg 1999, 28, 219.
9. Menezes, E. Text Ind Trade J 2002, 1, 35.
10. Yeo, S. Y.; Lee, H. J.; Jeong, J. S. H. Mater Sci 2003, 38, 2143.
11. Richard, P.; LeFloch, R.; Chamoux, C.; Pannier, M.; Espaze, E.; Richet, H. J Inf Dis 1994, 170, 377.
12. Yin, H. Q.; Langford, R.; Burrel, R. E. J Burn Care Rehab 1999, 20, 195.
13. Weiner, M. W.; Chen, H.; Gianellis, E. P.; Sogah, D. Y. J Am Chem Soc 1999, 121, 1615.
14. Aymonier, C.; Schlotterbeck, U.; Antonietti, L.; Zacharias, P.; Thomann, R.; Tiller, J. C.; Mecking, S. Chem Commun 2002, 2018.
15. Choi, S. H.; Lee, K. P.; Park, S. B. Nanotechnol Mesostruct Mater Stud Surf Sci Catal 2003, 146, 93.
16. Chen, Y.; Iroh, J. O. Chem Mater 1999, 11, 1218.
17. Zeng, R.; Rong, M. Z.; Zhang, M. Q.; Liang, H. C.; Zeng, H. M. Appl Surf Sci 2002, 187, 239.
18. Formes, T. D.; Yoon, R. J.; Keskkula, H.; Paul, D. R. Polymer 2001, 42, 9929.
19. Chae, D. W.; Oh, S. G.; Kim, B. C. J Polym Sci Part B: Polym Phys 2004, 42, 790.
20. Perkas, N.; Wang, Y.; Koltypin, Y.; Gedanken, A.; Chandrasekaran, S. Chem Commun 2001, 988.
21. Landau, M. V.; Vradman, L.; Herskowitz, M.; Koltypin, Y.; Gedanken, A. J Catal 2001, 201, 22.
22. Perkas, N.; Phan Minh, D.; Gallezot, P.; Gedanken, A.; Besson, M. J Appl Catal B 2005, 159, 121.
23. Salkar, R. A.; Jeevanandam, P.; Aruna, S. T.; Koltypin, Y.; Gedanken, A. J Mater Chem 1999, 9, 1333.
24. Pol, V. G.; Srivastava, D. N.; Palchik, O.; Palchik, V.; Slifkin, M. A.; Weiss, A. M.; Gedanken, A. Langmuir 2002, 18, 3352.
25. Chen, W.; Zhang, J.; Di, Y.; Wang, Z.; Fang, Q.; Cai, W. Appl Surf Sci 2003, 211, 280.
26. Ducamp-Sanguesa, C.; Herrera-Urbina, R.; Figlarz, M. J. Solid State Chem 1992, 100, 272.
27. Silvert, P. Y.; Herrera-Urbina, R.; Elhsissen, K. T. J Mater Chem 1997, 7, 293.
28. Carotenuto, G. Appl Organomet Chem 2001, 15, 344.
29. Vogel, A. I. Textbook of Quantitative Inorganic Analysis: Theory and Practice; Longman: London, 1962; p 256.
30. Kreibig, U.; Vollmer, M. Optical Properties of Metal Clusters; Springer: Berlin, 1995.
31. Itakura, T.; Torigoe, K.; Esumi, K. Langmuir 1995, 11, 4129.
32. Karpov, S. V.; Bas'ko, A. L.; Popov, A. K.; Slabko, V. V. Colloid J 2000, 62, 699.
33. Creigton, J. A.; Eadon, D. G. J Chem Soc Faraday Trans 1991, 87, 3881.
34. Taneja, P.; Ayyub, P.; Chandra, R. Phys Rev B 2002, 65, 245412.
35. Katagiri, G.; Ltonard, J. D.; Gustafson, T. L. Appl Spectrosc 1995, 49, 773.
36. Silman, O.; Lepp, A.; Kerker, M. Chem Phys Lett 1983, 100, 163.
37. Lee, A. S. L.; Li, Y.-S. J Raman Spectrosc 1994, 25, 209.
38. Gangopadhyay, P.; Kesavamoorthy, R.; Nair, K. G. M.; Dhanapani, R. J Appl Phys 2000, 88, 4975.